Ellipse packing in 2D cell tessellation: A theoretical explanation for Lewis's law and Aboav-Weaire's law

Kai Xu
Fisheries College, Jimei University, Xiamen, 361021, China
Email: kaixu@jmu.edu.cn
Phone: 86-592-6188860

Running title: Ellipse packing in 2D tessellation

Abstract

Background: To date, the theoretical bases of Lewis's law and Aboav-Weaire's law are still unclear.

Methods: Software R with package Conicfit was used to fit ellipses based on geometric parameters of polygonal cells of red alga *Pyropia haitanensis*.

Results: The average form deviation of vertexes from the fitted ellipse was 0±3.1 % (8,291 vertices in 1375 cells were examined). Area of the polygonal cell was 0.9±0.1 times of area of the ellipse's maximal inscribed polygon (EMIP). These results indicated that the polygonal cells can be considered as ellipse's inscribed polygons (EIPs) and tended to form EMIPs. This phenomenon was named as ellipse packing. Then, an improved relation of Lewis's law for a n-edged cell was derived

$$\text{cell area} = 0.5nabsin\left(\frac{2\pi}{n}\right)\left(1-\frac{3}{n^2}\right)$$

where, a and b are the semi-major axis and the semi-minor axis of fitted ellipse, respectively. This study also improved the relation of Aboav-Weaire's law

$$\text{number of neighboring cells} = 6+\frac{6-n}{n}\times\left(\frac{a}{b}+\frac{3}{n^2}\right)$$

Conclusions: Ellipse packing is a short-range order which places restrictions on the direction of cell division and the turning angles of cell edges. The ellipse packing requires allometric growth of cell edges. Lewis's law describes the effect of deformation from EMIP to EIP on area. Aboav-Weaire's law mainly reflects the effect of deformation from circle to ellipse on number of neighboring cells, and the deformation from EMIP to EIP has only a minor effect. The results of this study could help to simulate the dynamics of cell topology during growth.

PeerJ Preprints | https://doi.org/10.7287/peerj.preprints.27421v1 | CC BY 4.0 Open Access | rec: 9 Dec 2018, publ: 9 Dec 2018

Introduction

Three laws were generalized from observations on many natural and artificial two-dimensional (2D) structures: Euler's law, Lewis's law and Aboav-Weaire's law (Weaire & Rivier 1984). The latter two were first observed empirically by Lewis and Aboav with the original aims of understanding laws in biological structures and mechanisms of crystal growth, respectively (Aboav 1970; Lewis 1926; Lewis 1928; Weaire 1974). Although Lewis's law and Aboav-Weaire's law are very important for understanding the formation mechanisms of 2D structures, their theoretical explanations are still deficient (Mason et al. 2012; Weaire & Rivier 1984). Furthermore, to date, only one common feature was found in these 2D structures: the coordination number (the number of edges meeting at a vertex) is always three. This feature is a short-range order, and also the core mechanism mathematically determined that the average number of edges per cell is six (Graustein 1931).

Thallus of *P. haitanensis* is a single-layered prismatic cell sheet which is a mathematical consequence of 2D expansion on a plane by cell proliferation (Xu et al. 2017). Thus, *P. haitanensis* thalli can be simplified as 2D structures. When this study restrict attention to biological 2D structures, the word "cell" was used to represents the top and/or bottom faces of a prismatic cell. The dynamics of cell topology during growth make biological 2D structures even more complicated than other types of 2D structures. For examples, internal angles of *P. haitanensis* cells were concentrated in range of 100–140º by direction specific division and direction turning of cell edges, which suggested that the cells tended to form regular polygons (Xu et al. 2017). These observations hinted that there are undiscovered short-range orders in 2D structures. A recent study by Xu et al. (2018) found that the effective coverage area of ellipse-shaped exoskeletons of microalga *E. huxleyi* cells tended to approach the maximal area of EIP. Similar phenomenon was found in this study that the polygonal cells inclined to form EMIP. Based on this short-range order, the present study improved the relations of Lewis's law and Aboav-Weaire's law.

Materials and methods

Images of membranous thalli of *P. haitanensis* were analyzed using software Amscope Toupview 3.0. For each polygonal cell, the area (A_C), coordinates of center (X_{PC}, Y_{PC}) and vertices (X_V, Y_V) were measured. Software R (version 3.5.1) with package Conicfit was used to fit an ellipse based on the

PeerJ Preprints | https://doi.org/10.7287/peerj.preprints.27421v1 | CC BY 4.0 Open Access | rec: 9 Dec 2018, publ: 9 Dec 2018

coordinates of vertices of each polygonal cell (Fig. 1A) (Chernov et al. 2014). Five geometric parameters could be used to describe an ellipse, which include the semi-major axis a, semi-minor axis b, coordinates of center (X_{EC}, Y_{EC}), and angle of tilt of the major axis θ (Fig. 1B). On 2D geometry, five points determine a conic, for example, the ellipse. For polygons with five or more edges, X_{PC} and Y_{PC} were set as the initial values of coordinates of ellipse center to improve fitting. As for cells with only four edges, the coordinates of four vertices and four midpoints of edges were combined as a single data set to fit an ellipse as same as for cells with ≥ 5 edges. Then, the geometric parameters of the fitted ellipse were set as the initial values to fit the second ellipse for the coordinates of four vertices. The second ellipse was found to be the smallest one among all fitted ellipses, and which was used for analyzation. The reason of finding the smallest circumstanced ellipse for 4-edged polygonal cell was given in the next section. The area of ellipse (A_E) was calculated as

$$A_E = \pi ab \quad (1)$$

The area of the maximal inscribed polygon of ellipse (A_{MIP}) is

$$A_{MIP} = 0.5nab\sin\left(\frac{2\pi}{n}\right) \quad (2)$$

where n is the number of edges of inscribed polygon (Su 1987). The form deviation of vertex (*FD*) is

$$FD = \frac{D_{VC} - R}{R} \times 100\% \quad (3)$$

where D_{VC} is the distance between a vertex and the center of fitted ellipse (length of line VC)

$$D_{VC} = \sqrt{(X_V - X_{EC})^2 + (Y_V - Y_{EC})^2} \quad (4)$$

and R is the distance from the ellipse center to the cross point of the fitted ellipse and the line VC

$$R = \frac{ab}{\sqrt{(a\sin(\arctan(\tan\theta) - \delta))^2 + (b\cos(\arctan(\tan\theta) - \delta))^2}} \quad (5)$$

where δ is the angle between line VC and X-axis, the ranges of θ and δ are $[0, \pi)$ and $(-0.5\pi, 0.5\pi)$, respectively (Fig. 1B). R code and three examples for the above calculations can be found in supplementary files.

Results and discussion

Ellipse packing

The average number of cell edges was 6.0±0.9 (1,375 cells in 13 thalli were examined) which is consistent with previous studies in *P. haitanensis*, and many other organisms, and abiotic structures

PeerJ Preprints | https://doi.org/10.7287/peerj.preprints.27421v1 | CC BY 4.0 Open Access | rec: 9 Dec 2018, publ: 9 Dec 2018

(Gibson et al. 2006; Sánchez-Gutiérrez et al. 2016; Weaire & Rivier 1984; Xu et al. 2017). According to Euler's 2D formula, this kind of phenomenon was mathematically determined by a short-range geometric order, which is the coordination number of each vertex equal to three when different-sized cells tessellate a 2D plane (Graustein 1931; Weaire & Rivier 1984). The size differences between cells indicate that these biotic and abiotic 2D structures display long-range disorder, because unit cell has neither periodicity nor translational symmetry. Besides, the average number of cell edges quickly approached to six with exponential increase of cell number due to increase of body or tissue size. Thus, the above phenomenon can only be observed when a body or tissue contains a large number of cells (Graustein 1931; Lewis 1926; Weaire & Rivier 1984; Xu et al. 2017).

This study found that the vertices of a cell could be used to fit an ellipse with an average form deviation of 0±3.1 % (8,291 vertices in 1375 cells were examined, Table 1). Thus, polygonal cells of *P. haitanensis* were EIPs, which ensured that all the cells were convex polygons. The ratios of A_C/A_{MIP} ranged from 0.5 to 1.0 with an average value of 0.9±0.1 (Table 1), and 90% of the values concentrated in range of 0.78 to 0.97 (supplementary data S1), which indicated that cells preferred to reach the maximal area. Thus, the fitted ellipse should be the smallest circumstance ellipse of the polygonal cell, which was the reason to find the smallest ellipse for four-edged cells in this study. A recent study reported similar phenomenon on single-celled microalga *E. huxleyi* (Xu et al. 2018). *E. huxleyi* cells were fully covered by interlocked calcite exoskeletons, the specific geometric characteristics of exoskeletons resulted in that the effective coverage area of exoskeletons tended to reach the maximal area of inscribed polygon of ellipse-shaped exoskeletons.

The eccentric angle of neighboring vertices of EMIP is equal to $2\pi/n$ (Su 1987). Therefore, the eccentric angles of 6-edged EMIPs is 60º. Based on observations of direction specific divisions (resulted in equal-sized divisions) and division-associated direction changes of cell edges (concentrated internal angles in range of 100-140º), Xu et al. (2017) found that *P. haitanensis* cells preferred to form regular polygons. The more the polygonal cell close to a regular hexagon, the more the cell close to a spherical shape which could help to maintain force balance (Chen 2008; Ingber et al. 2014). Unbalanced forces could potentially result in unequal-sized cell division (Kiyomitsu 2015). However, equal-sized daughter cells can always be found in cell proliferation of *P. haitanensis* thalli (Xu et al. 2017).

PeerJ Preprints | https://doi.org/10.7287/peerj.preprints.27421v1 | CC BY 4.0 Open Access | rec: 9 Dec 2018, publ: 9 Dec 2018

Lewis's law

The average values of A_E, A_{MIP} and A_C increased with n, while the difference between average values of A_E and A_C was decreased (Fig. 2A). Except for $n > 8$, the average ratios of *a*/*b* were very stable regardless of values of n (Fig. 2B). Since A_{MIP} is $\frac{n}{2\pi}\sin\left(\frac{2\pi}{n}\right)$ times A_E (Su 1987), the ratio of A_{MIP}/A_E approaching to one with increase of n (Fig. 2C). Positive linear relationships were found between A_C and A_E (R^2=0.73, $P < 0.0001$, Fig. 2D), and between A_C and A_{MIP} (R^2=0.85, $P < 0.0001$, Fig. 2E). Thus, A_C can be calculated by the following empirical equation

$$A_C = 0.80A_{MIP} + 78.79 = 0.40nabsin\left(\frac{2\pi}{n}\right) + 78.79 \quad (6)$$

where, the maximal value of $nsin\left(\frac{2\pi}{n}\right)$ is

$$\lim_{n\to\infty} nsin\left(\frac{2\pi}{n}\right) = 2\pi \quad (7)$$

Because both $nsin\left(\frac{2\pi}{n}\right)$ and A_E increase with n (Fig. 2A,B), A_C also increase with n. This is consistent with Lewis's law, which suggests that A_C of a n-edged cell linearly related with n (Chiu 1995; Lewis 1926; Lewis 1928; Weaire & Rivier 1984). However, this study suggested the relationship between A_C and n is more complex than previous thoughts.

By equal-sized division, mitosis shall strongly disturb cell topology. Obviously, division should separate a cell along the direction of minor-axis of fitted ellipse, which makes daughter cells more close to EMIP (Fig. 3A). Nearly 150 years ago, Hofmeister proposed the similar speculation named long axis division (Hofmeister 1863). More complicated, however, Xu et al. (2017) found that divisions preferred to transect mother cells at midpoints of unconnected paired-edges. Afterward, directions of cell edges were changed to concentrate internal angle in range of 100–140°. Thus, the smallest number of edges per cell was four, and two equal-sized daughter cells were produced.

The ellipse packing is exactly a short-range order which could influence both local and global cell topology. The average axes of fitted ellipses and average number of edges were used to calculate the average variation of internal angles (Table1, Fig. 3A). Assuming a EMIP with 6 edges was divided along the minor axis of ellipse, then ellipse packing should turns all three polygonal cells around the new vertex into EMIPs (Fig. 3B). Thus, two daughter cells would be turned into two equal-sized maximal inscribed 5-gons, and the neighboring cell of both daughters would be turned into maximal inscribed 7-gon. The sum of three angles around the new vertex is 360º. Assuming the total disturbs on the three angles is minimum, based on least square method, the new internal angles around new vertexes in the neighboring cell would be decreased by 34.1º. Which gave an explanation to the observation that the turning angle was 40±6º (138 angles were examined) in the previous study by Xu et al. (2017). Meanwhile, those angles inherited from mother cells also need to be adjusted to obey ellipse packing (Fig. 3). Obviously, all these changes on angles must achieve by allometric growth of cell edges. The long axis division could decrease the disturb on cellular geometries and the payment to allometric growth of cell edges. Finally, from a global perspective, the combined effect of ellipse packing and the other short-range order (vertex coordination equal to three) turn all three angles around each vertex to 120º.

Aboav-Weaire's law

Aboav-Weaire's law describes that if m represents the average number of edges of cells surrounding a n-edged cell, then m is linearly related to $1/n$:

$$m = (6 - \beta) + \frac{6\beta + \mu_2}{n} \tag{8}$$

where, 6 is the average number of cell edges of 2D structures, β is a constant and μ_2 is related to the second moment of the edges of the n-edged cell (Weaire & Rivier 1984). The present study and previous study by Xu et al. (2017) showed that all cells tended to form regular polygons, which indicated that the internal angles tended to close to each other. According to Eq. (6), the cell area increase with n. The average internal angles of a n-edged cell is $\pi - \frac{2\pi}{n}$, which also increase with n. The sum of three angles around each vertex is 2π, which suggests that the average neighboring angles of the n-edged cell is decreasing with increase of n. Consequently, m, the average area and average internal angles of m cells tend to decrease with increase of n. Thus, Aboav-Weaire's law describes the representative level for a data set of $2n$ neighboring angles in the total data set of mn internal angles of neighboring cells.

Based on experimental studies, $\beta \approx 1.2$ was found to be conserved for several natural physical and biological structures (Aboav 1983; Aboav 1980; Mombach et al. 1990; Mombach et al. 1993). This number is very close to the average ratio of a/b of *P. haitanensis* cells (Table 1, Fig. 2B), and of oval-shaped exoskeletons (faces) of microalga *E. huxleyi* (Xu et al. 2018). In previous studies, μ_2 was assumed to be small (Edwards & Pithia 1994; Lambert & Weaire 1981). Regular hexagons could

PeerJ Preprints | https://doi.org/10.7287/peerj.preprints.27421v1 | CC BY 4.0 Open Access | rec: 9 Dec 2018, publ: 9 Dec 2018

monohedrally tessellate a plane (Grünbaum & Shephard 1987), such kind of tessellation also featured with ellipse packing and all vertexes have coordination equal to three. This indicates that when $n = \langle n \rangle = 6$, $\mu_2 = 0$, where $\langle n \rangle$ is the average number of cell edges. The observations of Aboav-Weaire's law in natural 2D structures suggest that the edge numbers of cells are uniformly distributed. The probability density function of m/n is

$$\mathrm{F}\left(\frac{\mathrm{m}}{\mathrm{n}}\right) = \begin{cases} 0 & \frac{m}{n} < \frac{4}{n} \ or \ \frac{m}{n} > \frac{10}{n} \\ \frac{n}{6} & \frac{4}{n} \leq \frac{m}{n} \leq \frac{10}{n} \end{cases} \tag{9}$$

The second moment of Eq. (9) is $\frac{3}{n^2}$, then μ_2 of a n-edged cell is $\frac{3}{n^2}(6-n)$, using Eq. (8) this study got

$$m = \left(6 - \frac{a}{b}\right) + \frac{\frac{6a}{b} + \frac{3(6-n)}{n^2}}{n} \tag{10}$$

where, a and b are the semi-major axis and semi-minor axis of fitted ellipse of a n-edged cell, respectively. The Eq. (10) can be rewritten as

$$m = 6 + \frac{6-n}{n} \times \left(\frac{a}{b} + \frac{3}{n^2}\right) \tag{11}$$

This equation could explain the monohedral tiling using equal-sized regular hexagons and 6-edged EMIPs (Fig. 3A top). As for m of *P. haitanensis* cells, the calculated values using Eq. (11) were very close to the real values by enumeration (Fig. 4A). The average difference between calculated m and real m was –0.1±0.3 (211 cells were examined). The a/b describes the deformation degree from circle to ellipse. Similarly, the present study assumed that the second moment of Eq. (9) describes the deformation degree from EMIP to EIP. This suggested the relation

$$\frac{3}{n^2} = 1 - \frac{\mathrm{A}_C}{\mathrm{A}_{MIP}} \tag{12}$$

which can be expressed as

$$\mathrm{A}_C = \mathrm{A}_{MIP}\left(1 - \frac{3}{n^2}\right) = 0.5nabsin\left(\frac{2\pi}{n}\right)\left(1 - \frac{3}{n^2}\right) \tag{13}$$

The results of this study strongly supported the above relation of Lewis's law (Fig. 4B). Meanwhile, the Eq. (11) can be rewritten as

$$m = 6 + \frac{6-n}{n} \times \left(\frac{a}{b} + 1 - \frac{\mathrm{A}_C}{\mathrm{A}_{MIP}}\right) \tag{14}$$

Due to μ_2 is very small, Aboav-Weaire's law could be approximately expressed as

$$m \approx 6 + \frac{6-n}{n} \times \frac{a}{b} \tag{15}$$

The calculated m using Eq. (11), Eq. (14) and Eq. (15) only showed minor differences (Fig. 4A, supplementary data S1).

Furthermore, for 2D structures, the combination of Lewis's law and Aboav-Weaire's law could derive a new law: big cells tend to surround by small cells, and vice versa. This law was frequently observed in many natural and artificial structures (Weaire & Rivier 1984). The results of this study could help to analyze the relation between areas of neighboring cells.

3D structures

Every prismatic cell of *P. haitanensis* thallus could be considered as a convex polyhedron with an average face number of eight. For multi- polyhedral-celled 3D structure with coordination number of four, the average face number is $\left(\frac{48}{35}\right)\pi^2 + 2\ (\approx 15.54)$ (Meijering 1953; Weaire & Rivier 1984). This number is very close to the average face number of 15.4 in single-polyhedral-celled microalga *E. huxleyi* with vertex coordination of three (Xu et al. 2018). The difference on average face number indicates that 2D and 3D structures are formed under different restrictions. A convex polyhedral cell is a sealed 3D structure which has a positive curvature at every vertex and obeys Euler's law. However, Euler's law does not set any restriction on 6-edged faces (Grünbaum & Motzkin 1963; Xu et al. 2018). Which suggests that a given 3D structure does not necessarily need to be a sealed structure even it obeys Euler's law. The closure of polyhedra could be considered as a basic level of uniform distribution of curvature. The face topology of polyhedra could be analyzed using software CaGe (Brinkmann et al. 2010).

Polygons with more than 6 edges induce locally negative curvature and with less than 6 edges induce positive curvature (Cortijo & Vozmediano 2007). Thus, the polyhedral cells of *E. huxleyi* only contains 4-gons, 5-gons and 6-gons which could help to maintain a full coverage on spherical surface (Xu et al. 2018). As for 2D tessellation using different-sized cells, the average edge number of 6 determined that the top and/or bottom faces of *P. haitanensis* cells contain four to ten edges (Table 1). Due to geometric limits, Lewis's law and Aboav-Weaire's law still valid for face topology of cells of *E. huxleyi* (Xu et al. 2018). Since Lewis's law only related to the semi-axes of fitted ellipse and the number of edges (Eq. 13), this law may be directly used for 3D structures. As for Aboav-Weaire's law, which may be able to generalize to 3D space with consideration of distribution of curvature at

PeerJ Preprints | https://doi.org/10.7287/peerj.preprints.27421v1 | CC BY 4.0 Open Access | rec: 9 Dec 2018, publ: 9 Dec 2018

vertexes.

Conclusion

This study found that polygonal cells of *P. haitanensis* inclined to form EMIPs. This phenomenon was named as ellipse packing, which could be applied in simulation of dynamics of cell topology during growth. Improved relations of Lewis's law and Aboav-Weaire's law were derived and tested using the geometric parameters of fitted ellipses and the number of cell edges. The present study suggested that Lewis's law and Aboav-Weaire's law are nonlinear relations, the former describes the deformation effect of EMIP on area, and the latter describes the deformation effects of circle (major effect) and EMIP (minor effect) on number of neighboring cells. This study also gave a mathematical explanation for long axis division. Further works are needed to test our results in other 2D structures.

Acknowledgements

The author thank Miss Zhixue Chen for her assistance on collect geometric data of cells. I thank my mother Yuntao Yan and my wife Huimin Cheng for their wholehearted supports.

References

Aboav D. 1983. The arrangement of cells in a net. II. *Metallography* 16:265-273.

Aboav DA. 1970. The arrangement of grains in a polycrystal. *Metallography* 3:383-390.

Aboav DA. 1980. The arrangement of cells in a net. *Metallography* 13:43-58.

Brinkmann G, Friedrichs OD, Lisken S, Peeters A, and Van Cleemput N. 2010. CaGe—a virtual environment for studying some special classes of plane graphs—an update. *Match Communications In Mathematical And In Computer Chemistry* 63:533-552.

Chen CS. 2008. Mechanotransduction - a field pulling together? *Journal of Cell Science* 121:3285-3292. 10.1242/jcs.023507

Chernov N, Huang Q, and Ma H. 2014. Fitting quadratic curves to data points. *British Journal of Mathematics & Computer Science* 4:33-60.

Chiu S. 1995. Aboav-Weaire's and Lewis' laws—A review. *Materials characterization* 34:149-165.

Cortijo A, and Vozmediano MAH. 2007. Effects of topological defects and local curvature on the electronic properties of planar graphene. *Nuclear Physics B* 763:293-308. 10.1016/j.nuclphysb.2006.10.031

Edwards S, and Pithia K. 1994. A note on the Aboav-Weaire law. *Physica A: Statistical Mechanics and its Applications* 205:577-584.

Gibson MC, Patel AB, Nagpal R, and Perrimon N. 2006. The emergence of geometric order in proliferating metazoan epithelia. *Nature* 442:1038-1041.

Graustein W. 1931. On the average number of sides of polygons of a net. *Annals of*

Mathematics:149-153.

Grünbaum B, and Motzkin TS. 1963. The number of hexagons and the simplicity of geodesics on certain polyhedra. *Canadian Journal of Mathematics* 15:744-751.

Grünbaum B, and Shephard GC. 1987. Tilings and patterns. *The American Mathematical Monthly* 95:xii+446.

Hofmeister W. 1863. Zusatze und Berichtigungen zu den 1851 veroffentlichen Untersuchungen der Entwicklung hoherer Kryptogamen. *Jahrbucher für Wissenschaft und Botanik* 3:259-193.

Ingber DE, Wang N, and Stamenovic D. 2014. Tensegrity, cellular biophysics, and the mechanics of living systems. *Reports on Progress in Physics* 77:046603. 10.1088/0034-4885/77/4/046603

Kiyomitsu T. 2015. Mechanisms of daughter cell-size control during cell division. *Trends in Cell Biology* 25:286-295.

Lambert C, and Weaire D. 1981. Theory of the arrangement of cells in a network. *Metallography* 14:307-318.

Lewis FT. 1926. The effect of cell division on the shape and size of hexagonal cells. *The Anatomical Record* 33:331-355.

Lewis FT. 1928. The correlation between cell division and the shapes and sizes of prismatic cells in the epidermis of cucumis. *The anatomical record* 38:341-376.

Mason JK, Ehrenborg R, and Lazar EA. 2012. A geometric formulation of the law of Aboav–Weaire in two and three dimensions. *Journal of Physics A: Mathematical and Theoretical* 45:065001. 10.1088/1751-8113/45/6/065001

Meijering JL. 1953. Interface area, edge length, and number of vertices in crystal aggregates with random nucleation. *Philips Res Rep*.

Mombach J, Vasconcellos M, and de Almeida RM. 1990. Arrangement of cells in vegetable tissues. *Journal of Physics D: Applied Physics* 23:600.

Mombach JCM, de Almeida RM, and Iglesias JR. 1993. Mitosis and growth in biological tissues. *Physical Review E* 48:598.

Sánchez-Gutiérrez D, Tozluoglu M, Barry JD, Pascual A, Mao Y, and Escudero LM. 2016. Fundamental physical cellular constraints drive self-organization of tissues. *EMBO Journal* 35:77-88. 10.15252/embj.201592374

Su H. 1987. The characteristics of maximum inscribed and minimum circumscribed polygons of ellipse. *Teaching Mathematics* 6:22-26.

Weaire D. 1974. Some remarks on the arrangement of grains in a polycrystal. *Metallography* 7:157-160.

Weaire D, and Rivier N. 1984. Soap, cells and statistics—random patterns in two dimensions. *Contemporary Physics* 25:59-99. 10.1080/00107518408210979

Xu K, Hutchins D, and Gao K. 2018. Coccolith arrangement follows Eulerian mathematics in the coccolithophore *Emiliania huxleyi*. *PeerJ* 6:e4608. 10.7717/peerj.4608

Xu K, Xu Y, Ji D, Chen T, Chen C, and Xie C. 2017. Cells tile a flat plane by controlling geometries during morphogenesis of *Pyropia* thalli. *PeerJ* 5:e3314. 10.7717/peerj.3314

Table 1 Parameters of polygonal cells and fitted ellipses.

Parameters	Mean±SD	Range	*n*
Average number of cell edges (n)	6.0±0.9	4–10	1,375
Form deviation (FD, %)	0±3.1	–13.9–20.6	8,291
Fitted semi-major-axis (a, μm)	19.9±2.8	13.9–37.2	1,375
Fitted semi-minor-axis (b, μm)	15.3±1.7	9.3–21.8	1,375
a/b	1.3±0.2	1.0–2.7	1,375
Area of fitted ellipse (A_E, μm^2)	961.8±195.3	506.2–2016.9	1,375
Area of the maximal inscribed polygon of fitted ellipse (A_{MIP}, μm^2)	788.2±172.0	343.2–1,667.9	1,375
Area of cell (A_C, μm^2)	706.0±149.0	303.9–1,512.6	1,375
A_C/A_{MIP}	0.9±0.1	0.5–1.0	1,375

PeerJ Preprints | https://doi.org/10.7287/peerj.preprints.27421v1 | CC BY 4.0 Open Access | rec: 9 Dec 2018, publ: 9 Dec 2018

Figure 1 Geometry of polygonal cell and fitted ellipse. (A) Coordinates of vertexes of a polygonal cell and fitted ellipse. The ellipse was plotted using Software R with package Conics (Chernov et al. 2014). (B) A diagram shows semi-major-axis a, semi-minor-axis b, angle between line VC and X-axis δ, angle of tilt of the major axis θ, distance between center of ellipse and vertex of polygonal cell D_{VC}, distance from center of ellipse to the cross point of line VC and fitted ellipse R.

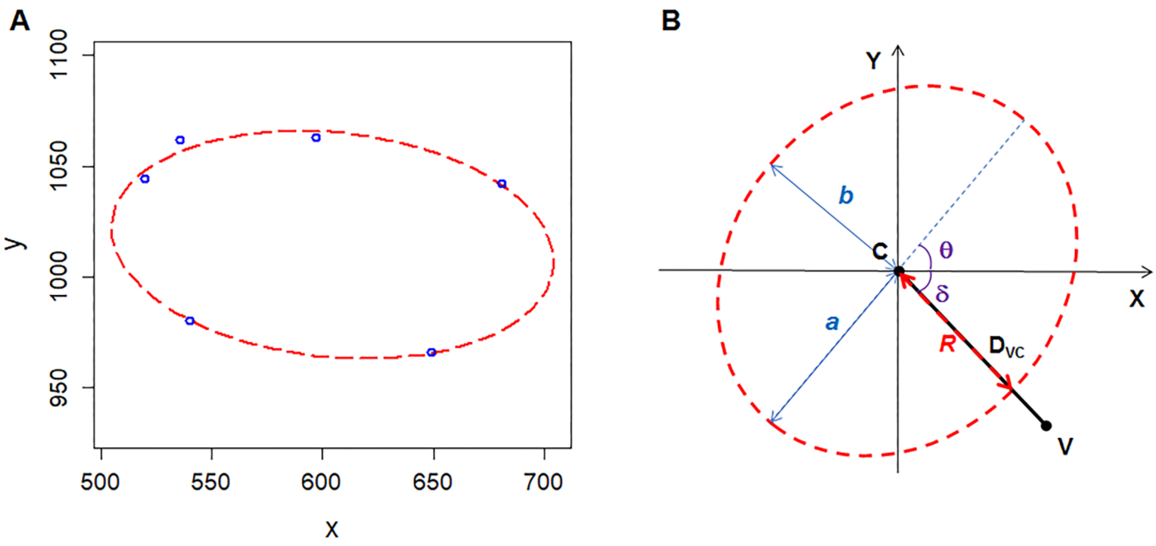

PeerJ Preprints | https://doi.org/10.7287/peerj.preprints.27421v1 | CC BY 4.0 Open Access | rec: 9 Dec 2018, publ: 9 Dec 2018

Figure 2 Relationships between n, A_C, A_{MIP} and A_E. (A) Relationships between number of cell edges n, area of cell A_C, area of the maximal inscribed polygon A_{MIP}, and area of fitted ellipse A_E. Big symbols represent the average values of A_C, A_{MIP} and A_E, while small symbols represent the raw data (1,375 cells were analyzed). (B) Relationship between n and ratio of *a*/*b*. (C) Relationship between n and ratio of A_{MIP}/A_E. (D) Relationship between A_C and A_{MIP} (1,375 cells were analyzed). (E) Relationship between A_C and A_E (1,375 cells were analyzed).

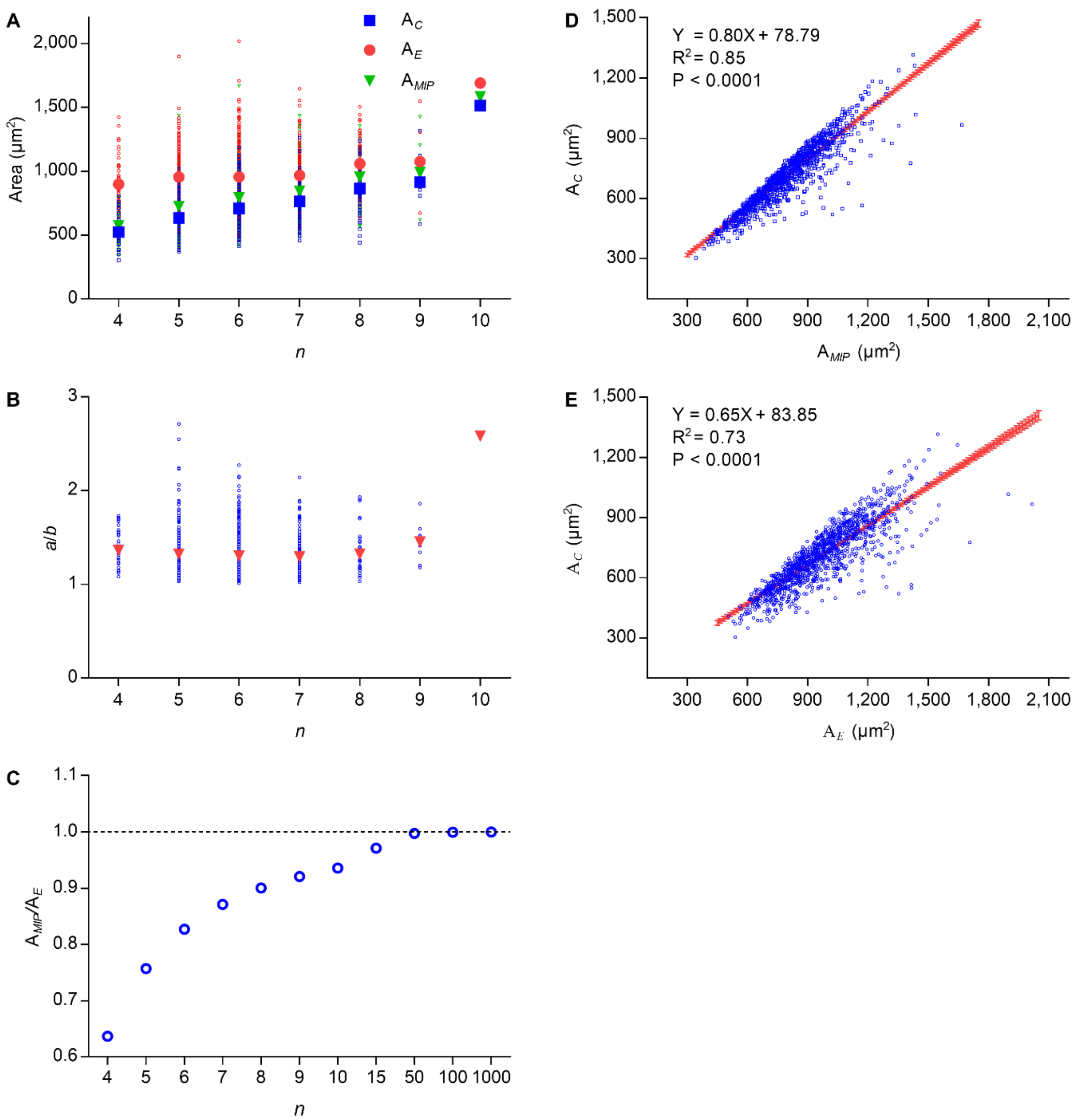

PeerJ Preprints | https://doi.org/10.7287/peerj.preprints.27421v1 | CC BY 4.0 Open Access | rec: 9 Dec 2018, publ: 9 Dec 2018

Figure 3 Cell division obeys ellipse packing. (A) Red dash line represents that division of the maximal inscribed 6-gon divided the cell along the minor axis of ellipse, and produced two equal-sized daughters. Blue dash line shows that an edge was separated by a new vertex which produced three new angles (bottom). (B) Ellipse packing would turns the daughters into maximal inscribed 5-gons (top left) by allometric growth of cell edges, meanwhile the neighboring 7-gon also need to be turned into EMIP (top right). To minimize the total disturbs on the three angles, the turning angle in neighboring cell should be 34.1º (bottom). (C) Three angles around each vertex tended to be 120º. The ratios of *a*/*b* of all ellipses were set to an average value of 1.3.

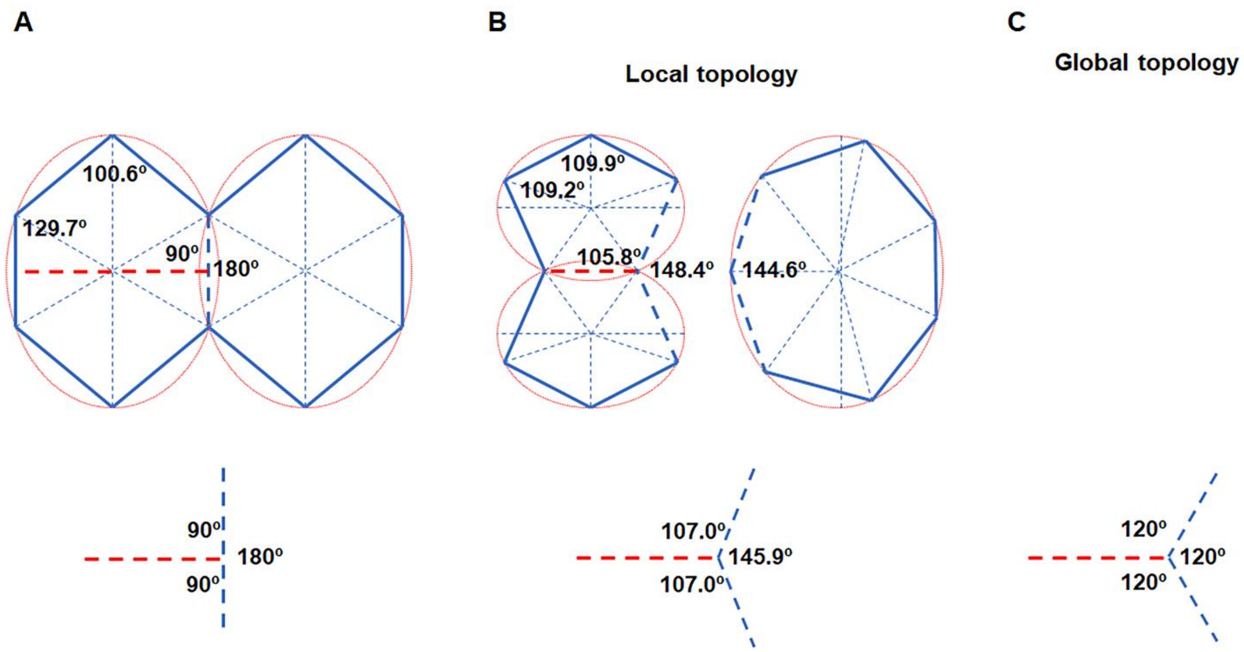

PeerJ Preprints | https://doi.org/10.7287/peerj.preprints.27421v1 | CC BY 4.0 Open Access | rec: 9 Dec 2018, publ: 9 Dec 2018

Figure 4 Examinations of relations of Lewis's law and Aboav-Weaire's law. (A) Relationship between real and calculated number of neighboring cells m of a n-edged cell (211 cells were examined). The Eq. (11), (14) and (15) were used to calculate m. (B) Relationship between real and calculated area of a n-edged polygonal cell (1,375 cells were examined). The Eq. (13) was used to calculated cell area.

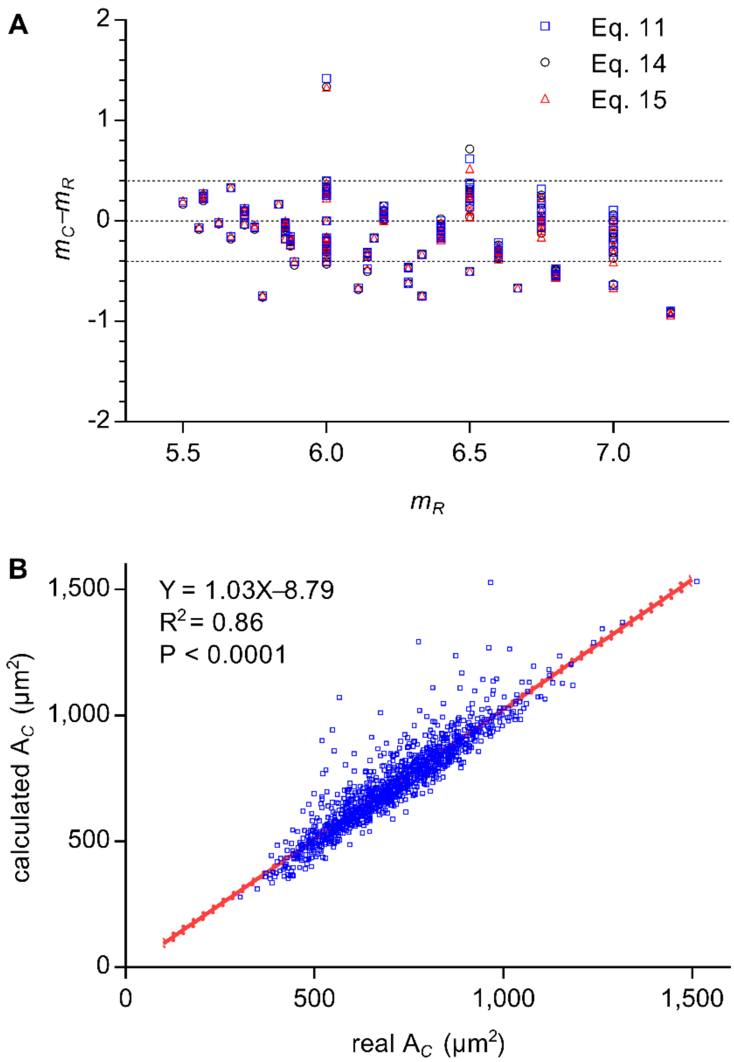

PeerJ Preprints | https://doi.org/10.7287/peerj.preprints.27421v1 | CC BY 4.0 Open Access | rec: 9 Dec 2018, publ: 9 Dec 2018